Supplementary Information: Flash Sintering Incubation Kinetics

K. S. N. Vikrant,[1] Han Wang,[1] Aniruddha Jana,[1]

Haiyan Wang,[1,2] and R. Edwin García[1,*]

March 25, 2020

1: School of Materials Engineering,

Purdue University, West Lafayette, IN 47907, USA.

2: School of Electrical and Computer Engineering,

Purdue University, West Lafayette, IN 47907, USA.

∗: Contact author. phone:(765) 463-7801; email: redwing@purdue.edu

Supplementary Experimental Setup

Plan-view TEM specimens of flash sintered 3YSZ samples for an applied electric field of 60 V/cm were prepared through conventional approach [1], which includes manual grinding, polishing, dimpling and final polishing in an ion milling system (PIPS II, Gatan). A FEI TALOS TEM/STEM with ChemiS-TEM technology (X-FEG and SuperX EDS with four silicon drift detectors) operated at 200 kV was used in this study for microstructure characterization and energy-dispersive X-ray spectroscopy (EDS) chemical mapping.

Supplementary Numerical Implementation

The two-dimensional green body microstructure (see Supplementary Figure 1) was computationally generated from a pool of circular particles with sizes following a lognormal size distribution of mean diameter of 100nm, and standard deviation of 30nm. For two-dimensional green body simulations, the furnace and sample temperature was initialized to 25°C, while the furnace temperature was ramped up at a constant heating rate of 10K/min. YSZ properties are summarized in Supplementary Table 1. Initial $[V_O^{\cdot\cdot}]$ and $[Y'_{Zr}]$ were set to its experimental equilibrium values [2,3], and set to zero in porous regions. Electrically, the right edge of the simulation domain was grounded, and a fixed voltage was applied to the left edge. Equation set 2, Equations 3 and 4 in the main text, were solved across a 1μm $\times$ 1μm simulation domain, and discretized into a 1000×1000 finite volume mesh. The partial differential equations were implemented in FiPy [4]. The relative tolerance for convergence was set to 1×10^{-8}. Each simulation took on the order of 36 hrs of wall time to complete.

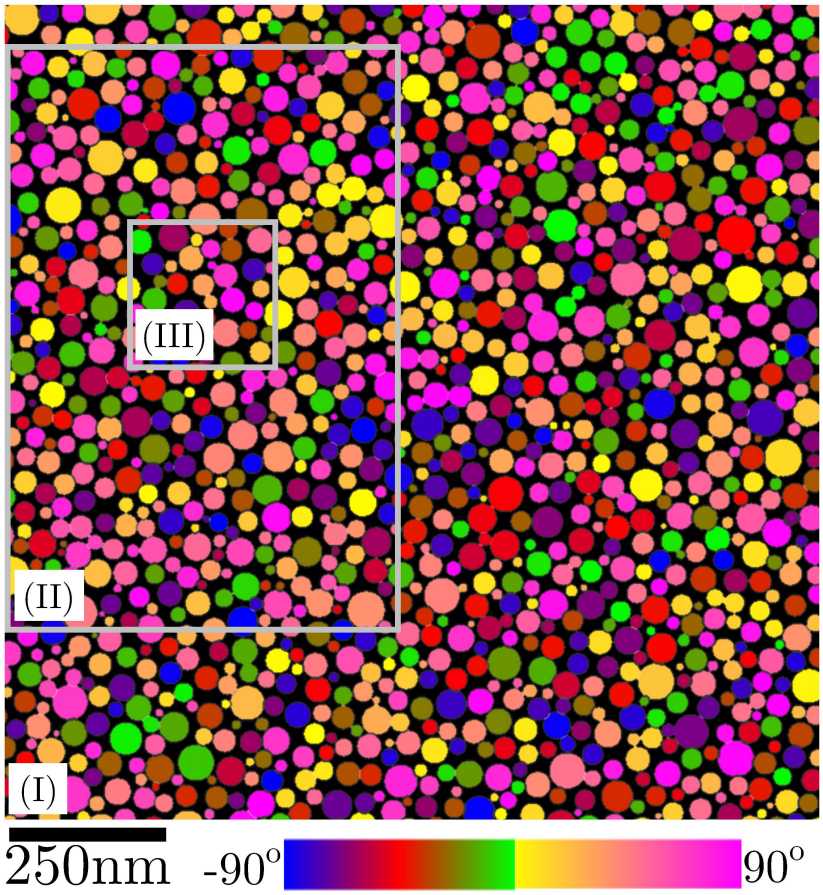

Supplementary Figure 1: Simulation setup for EFAS of a green body sample in a furnace. The particles of the green body are perfectly circular, possessing a lognormal size distribution of average diameter 100nm, and standard deviation 30nm, with 33% porosity as reported by the manufacturer [5]. The black region corresponds to the porosity. The right edge of simulation domain was set to be electrically grounded, and a fixed voltage was applied to the left edge. The furnace temperature is increased at a constant heating rate of 10K/min.

Supplementary Table 1: Summary of physical parameters used in flash sintering calculations for 3YSZ.

Parameter	Symbol	Value	Units	Ref.
Oxygen vacancies ionic valence	Z_O	2	–	–
Yttrium defects ionic valence	Z_Y	-1	–	–
Segregation energy of oxygen vacancies to grain boundary	$f^d_{V_O^{\cdot\cdot}} - f^{\times}_{V_O^{\cdot\cdot}}$	-0.5	eV	[6]
Segregation energy of oxygen vacancies to surface	$f^v_{V_O^{\cdot\cdot}} - f^{\times}_{V_O^{\cdot\cdot}}$	-0.5	eV	[6]
Segregation energy of yttrium defects to grain boundary	$f^d_{Y'_{Zr}} - f^{\times}_{Y'_{Zr}}$	0.0	eV	[7]
Segregation energy of yttrium defects to surface	$f^v_{Y'_{Zr}} - f^{\times}_{Y'_{Zr}}$	0.0	eV	[7]
Interaction parameter	$\Omega_{Y'_{Zr}V_O^{\cdot\cdot}}$	-0.13	eV	[8]
Atomic volume of Zirconia	ν	3.6×10^{-29}	m^3/atom	–
Latent heat of fusion	$\Delta H^{\times\rightarrow v}$	3.5×10^9	J/m^3	–
Melting temperature	T_m	2988	K	–
Order-disorder interfacial energy	$\gamma_{\times d}$	0.6	J/m^2	[9]
Structural coupling parameter	$s_1 = \frac{2a\alpha}{\Delta\theta_{max}}$	4.6	J/m^2	[10]
Structural coupling parameter	s_2	0.008	J/m	[10]
Interfacial thickness between order-disorder phases	$\delta_{\times d}$	1	nm	–
Interfacial thickness between disorder-porous phases	δ_{dv}	1	nm	–
Interfacial thickness between order-porous phases	$\delta_{\times v}$	1	nm	–
Energy barrier between order-disorder phases	$w_{\times d} = \frac{3\gamma_{\times d}}{\delta_{\times d}}$	1.8×10^9	J/m^3	[11]
Energy barrier between disorder-porous phases	$w_{dv} = \frac{3\gamma_{dv}}{\delta_{dv}}$	2.4×10^9	J/m^3	[11]
Energy barrier between order-porous phases	$w_{\times v} = \frac{3\gamma_{\times v}}{\delta_{\times v}}$	2.4×10^9	J/m^3	[11]
Gradient energy coefficient of order-disorder interface	$\alpha_\times = 6\gamma_{\times d}\delta_{\times d}$	1.8×10^{-9}	J/m	[11]
Gradient energy coefficient of disorder-porous interface	$\alpha_v = 6\gamma_{dv}\delta_{dv}$	2.4×10^{-9}	J/m	[11]
Gradient energy coefficient of order-porous interface	$\alpha_{\times v} = 6\gamma_{\times v}\delta_{\times v},$	2.4×10^{-9}	J/m	[11]
Gradient energy coupling coefficient of order-porous interface	$\alpha_d = \alpha_\times + \alpha_v - \alpha_{\times v}$	1.8×10^{-9}	J/m	[11]
Kinetic coefficient for crystalline transformation	$M_{\eta_\times}$	3.6×10^{-8}	m/Js^3	–
Kinetic coefficient for orientation transformation	M_θ	3.6×10^{-7}	m/Js^3	–
Mobility of porous phase	M_{η_v}	7.02×10^{-28}	m^5/Js	–
Relative dielectric permittivity of YSZ	ϵ_r	32	–	[12]
Relative dielectric permittivity of pores	ϵ_r	1	–	–
Emissivity of YSZ green body	e	0.6	–	–
Heat capacity of YSZ	c_σ	56.47	J/mol K	[12]
Stefan-Boltzmann constant	σ_e	5.67×10^{-8}	W/m	–

Supplementary References

[1] Rao, D. V. S., Muraleedharan, K. & Humphreys, C. J. TEM specimen preparation techniques. *Microscopy: Science, Technology, Applications and Education* 1232–1242 (2010).

[2] Naik, K. S., Sglavo, V. M. & Raj, R. Field assisted sintering of ceramic constituted by alumina and yttria-stabilized zirconia. *J. Eu. Ceram. Soc.* **76**, 2435–2442 (2014).

[3] Downs, J. A. & Sglavo, V. M. Electric field assisted sintering of cubic zirconia at 390°C. *J. Am. Ceram. Soc.* **96**, 1342–1344 (2013).

[4] Guyer, J. E., Wheeler, D. & Warren, J. A. FiPy: Partial differential equations with python. *Comput. Sci. Eng.* **11**, 615 (2009).

[5] Vaz, M. F. & Fortes, M. A. Grain size distribution: The lognormal and the gamma distribution functions. *Scripta Metallurgica* **22**, 35–40 (1988).

[6] Xia, X., Catlow, C. R. A. & Oldman, R. Computational modeling study of bulk and surface of yttria-stabilized cubic zirconia. *Chem. Mater.* **21**, 3576–3585 (2009).

[7] Romero, R. L. G., Melendez, J. J., García, D. G., Cumbrera, F. L. & Rodriguez, A. D. Segregation to the grain boundaries in YSZ bicrystals: A molecular dynamics study. *Solid Sate Ionics* **237**, 8–15 (2013).

[8] Pornprasertsuk, R., Ramanarayanan, P., Musgrave, C. B. & Prinz, F. B. Predicting ionic conductivity of solid oxide fuel cell electrolyte from first principles. *J. Appl. Phys.* **98**, 103513 (2005).

[9] Shibata, N., Oba, F., Yamamoto, T. & Ikuhara, Y. Structure, energy and solute segregation behavior of [110] symmetric tilt grain boundaries in yttria-stabilized cubic zirconia. *Philos. Mag. Lett.* **84**, 2381–2415 (2004).

[10] Warren, J. A., Kobayashi, R., Lobkovsky, A. E. & Carter, W. C. Extending phase field models of solidification to polycrystalline materials. *Acta. Mater.* **51**, 6035–6058 (2003).

[11] Boettinger, W. J., Warren, J. A., Beckermann, C. & Karma, A. Phase-field simulation of solidification. *Annu. Rev. Mater. Res.* **32**, 163–194 (2002).

[12] Thompson, D. P. & Dickins, A. M. The dielectric properties of zirconia. *J. Mater. Sci.* **27**, 2267–2271 (1992).